Transfer Across Random versus Deterministic Fractal Interfaces

M. Filoche[1] and B. Sapoval[1,2]

[1]*Laboratoire de Physique de la Matière Condensée, C.N.R.S. Ecole Polytechnique, 91128 Palaiseau, France*
[2]*Centre de Mathématiques et de leurs Applications, Ecole Normale Supérieure, 94140 Cachan, France*

(Received 28 September 1999)

A numerical study of the transfer across random fractal surfaces shows that their responses are very close to the response of deterministic model geometries with the same fractal dimension. The simulations of several interfaces with prefractal geometries show that, within very good approximation, the flux depends only on a few characteristic features of the interface geometry: the lower and higher cutoffs and the fractal dimension. Although the active zones are different for different geometries, the electrode responses are very nearly the same. In that sense, the fractal dimension is the essential "universal" exponent which determines the net transfer.

PACS numbers: 61.43.Hv, 41.20.Cv, 82.65.Jv

Many random processes, such as aggregation, diffusion, fracture, and percolation, build fractal objects [1,2]. Fractal geometry essentially describes hierarchical structures [3]. If properties of these random systems depend on the hierarchical character of their geometry, then the study of a deterministic structure with the same fractal dimension may provide a good approximation of the random system properties [4]. The question is significant since fractal and prefractal geometries are widely used in mathematical approaches or numerical simulations as a convenient model of irregularity. They are also more simply addressed by algebraic calculations and incorporated into numerical models for computer simulation. It is then an important matter to decide whether simple deterministic, *artificial,* fractals could help determine the properties of random, *natural,* fractals [5,6]. In particular, it is a question whether experiments performed on model fractal geometries [7] may help understand the behavior of real complex structures.

The property which is discussed here is the Laplacian transport to and across irregular and fractal interfaces. Such transport phenomena are often encountered in nature or in technical processes: properties of rough electrodes in electrochemistry, steady-state diffusion towards irregular membranes in physiological processes, the Eley-Rideal mechanism in heterogeneous catalysis in porous catalysts, and in NMR relaxation in porous media. In each of these examples, the interface presents a *finite* transfer rate, similar to a redox reaction, or a finite permeability, or reaction rate which is due to specific physical or chemical processes.

The mathematical formulation of the problem is simple. One considers the current flowing through an electrochemical cell as shown in Fig. 1. The current $\vec{J}$ is proportional to the Laplacian field $\vec{\nabla} V$, which can be viewed as an electrostatic field in electrochemistry, or a particle concentration field in diffusion problems. Then the flux and field are related by classical equations of the type $\vec{J} = -\sigma \vec{\nabla} V$, where σ is the electrolyte conductivity (or particle diffusivity in diffusion or heterogeneous catalysis). The conservation of this current throughout the bulk yields the Laplace equation for the potential V:

$$\mathrm{div}(-\sigma \vec{\nabla} V) = 0 \Rightarrow \Delta V = 0 . \tag{1}$$

The boundary presents a finite resistance r to the current flow. In the simplest case, this resistance can be expressed by a linear relation linking the current density across the boundary to the potential drop across that boundary. The local flux and potential drop are then linked by transport coefficients, such as the faradaic resistance in electrochemistry, the membrane permeability in physiological processes, or again the surface reactivity in catalysis. If one assumes that the outside of the irregular boundary is at zero potential, current conservation at the boundary leads to the following relation:

$$\vec{J} \cdot \vec{n} = -\frac{V}{r} , \tag{2}$$

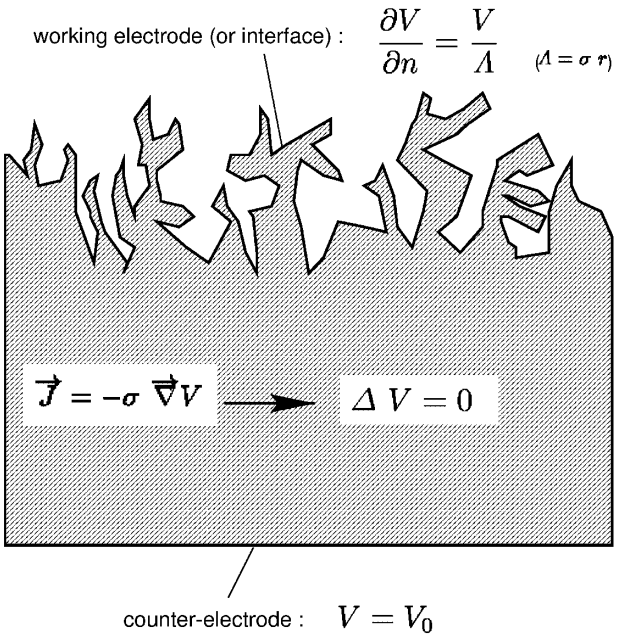

FIG. 1. Schematic representation of an electrochemical cell.

 0031-9007/00/84(25)/5776(4)$15.00

or

$$\frac{\partial V}{\partial n} = \frac{V}{\Lambda} \quad \text{with } \Lambda = \sigma r\,. \tag{3}$$

The parameter Λ is homogeneous to a length. Given the geometry, the value of this parameter determines the behavior of the system [8,9]. The overall response of such a system is measured by one scalar quantity, its impedance Z_{tot}, which is the ratio between the applied potential and the total flux:

$$Z_{\text{tot}} = \frac{V_0}{\Phi}\,. \tag{4}$$

The contribution of the finite interface resistivity to this global impedance is given by a "spectroscopic" impedance, defined as $Z_{\text{spect}} = Z_{\text{tot}} - Z_0$, Z_0 being the impedance of the cell with zero interface resistivity [9]. The main result discussed below is that the electrode impedance Z_{spect} is nearly independent of the random character of the fractal interface, even though the regions where the current is concentrated are very different. This is found from a numerical comparison between impedances of deterministic and random electrodes with the same fractal dimension. Two cases are studied: (a) deterministic and random von Koch electrodes (dimension $D_f = \ln 4/\ln 3$); (b) a deterministic electrode of dimension $D_f = 4/3$ and a self-avoiding random walk geometry with the same dimension.

The deterministic von Koch curve, or classical snowflake curve, is obtained by dividing a line segment into three equal parts, removing the central segment, and replacing it by two other identical segments which form an equilateral triangle [3]. A random von Koch curve can be defined simply by choosing randomly the side of the segment where the triangle is created at each step of the building process. The cases where two triangles would touch are excluded as they correspond to a geometrical pathology that does not represent the randomness of a natural system. The result of this process is shown in Fig. 2. After three or more generations, it looks more like a realistic random boundary than a simple mathematical curve. It is then possible to automatically generate different boundaries that have the same fractal dimension and the same perimeter. By definition, fractal geometries exhibit a large scale of lengths. For instance, at the sixth generation, the ratio between the smallest feature l (smaller cutoff) of the irregular boundary and the diameter L (larger cutoff) is $3^6 = 729$ while the length of the perimeter is $L_p = 4^6 l = 4096l$. Computing on a regular grid within such geometries would be very memory and time consuming. A finite element method is then used. The standard variational formulation of the problem is discretized with a triangular mesh, obtained from a Delaunay-Voronoï tessellation and P_1-Lagrange interpolation. The linear system obtained in such a way is solved by using the Cholesky method, from the Finite Element Library MODULEF [10]. Examples of meshes with a sixth generation boundary are shown in Fig. 3.

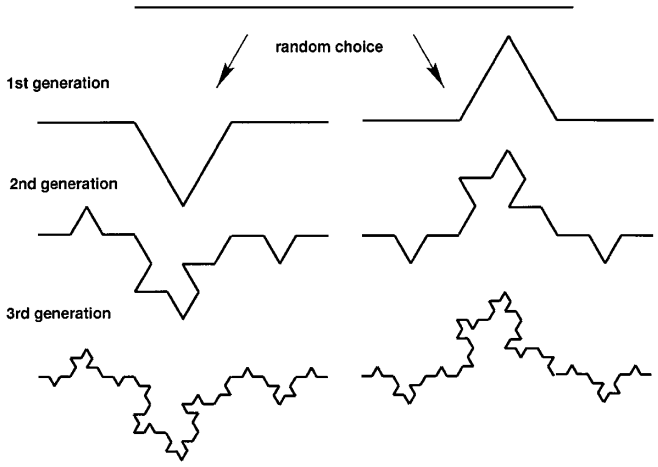

FIG. 2. The building process of random von Koch curves. The same random process can create various interface topographies. They share the same size, the same perimeter, and the same fractal dimension.

Computations were carried out for the two deterministic boundary geometries and the two random geometries of generation six shown in Fig. 4. The figure presents the

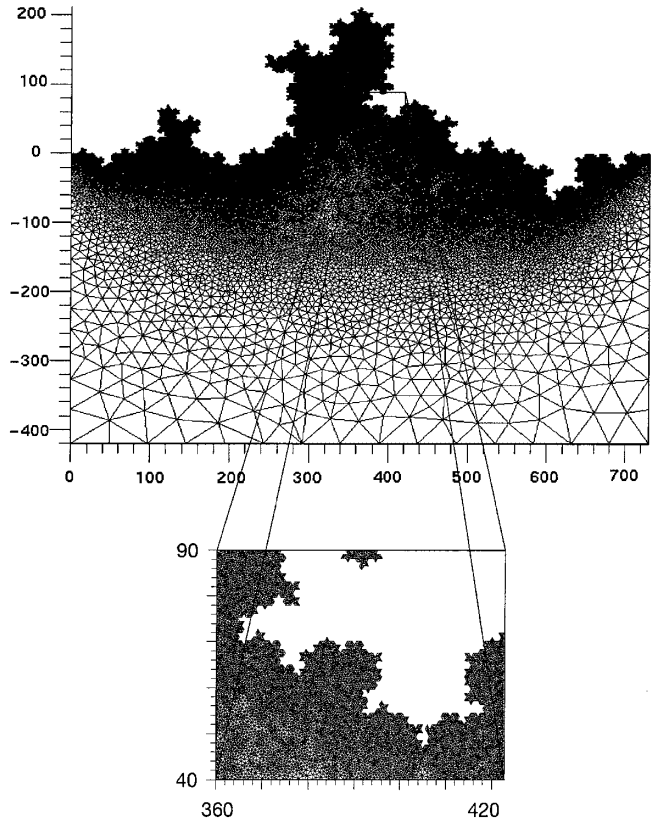

FIG. 3. A finite element mesh for the sixth generation von Koch random electrode. Top: An example of a finite element mesh for the sixth generation interface. Bottom: Local zoom of the mesh.

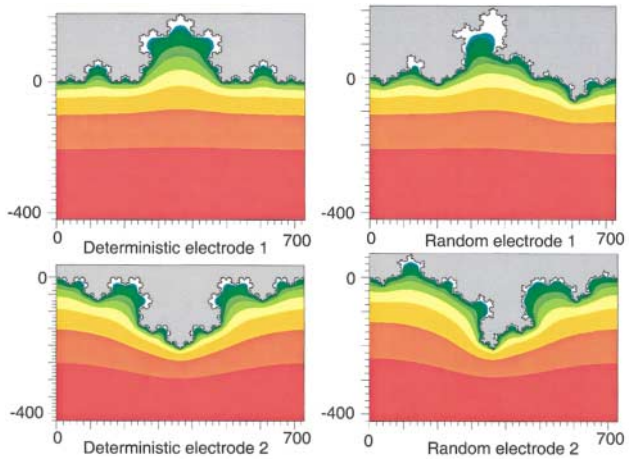

FIG. 4 (color). Isopotential curves for von Koch deterministic and random electrodes with $\Lambda = 0$ (Dirichlet boundary condition). The equipotential lines are the lines separating regions of exponentially decreasing potential: $V = 1$ at the bottom then $1/2$, $1/4$, $1/8, \ldots$. The current density is proportional to the gradient of the potential. The current is then large in regions where the curves are close. Note that the current flows through the interface primarily at the tips. These active zones are found at very different locations for different electrodes.

isopotential curves for $\Lambda = 0$. Since the current density is proportional to the gradient of the potential, one can detect regions of large current density from the distance between two consecutive isopotential curves: the closer the equipotentials, the larger the current density. As expected, most of the current flows through the irregular interface at the tips. This gives a very different current map for each geometry. Therefore, for the different electrodes the active zones are very different.

The second type of electrodes to be compared is shown in Fig. 5. The top figure shows the second generation of a deterministic fractal electrode with dimension $D_f = \ln 16/\ln 8 = 4/3$ while the bottom represents a particular self-avoiding walk with the same $4/3$ fractal dimension. Both electrodes have the same perimeter and the same smaller cutoff. Here, even more than above, the active zones are totally different.

For each geometry, the impedances have been computed for an extended range of the surface resistivity r. The results are shown in Fig. 6 for two categories of geometries: sixth generation of von Koch electrodes and the two electrodes of Fig. 5. The parameter $\Lambda/l = \sigma r/l$ ranges between 1 and 10^5 for generation six and between 10^{-1} and 5×10^3 for the second type. The limitation of the range is due to limitations in computer time and memory.

It is striking that, despite very different current distribution in the bulk and at the interface, the impedances are very close for all values of the surface resistivity. The behavior of different interfaces are nearly indistinguishable: random and deterministic interfaces behave in the same manner. This could be considered as a partial answer to the question "Can one hear the shape of an electrode?"

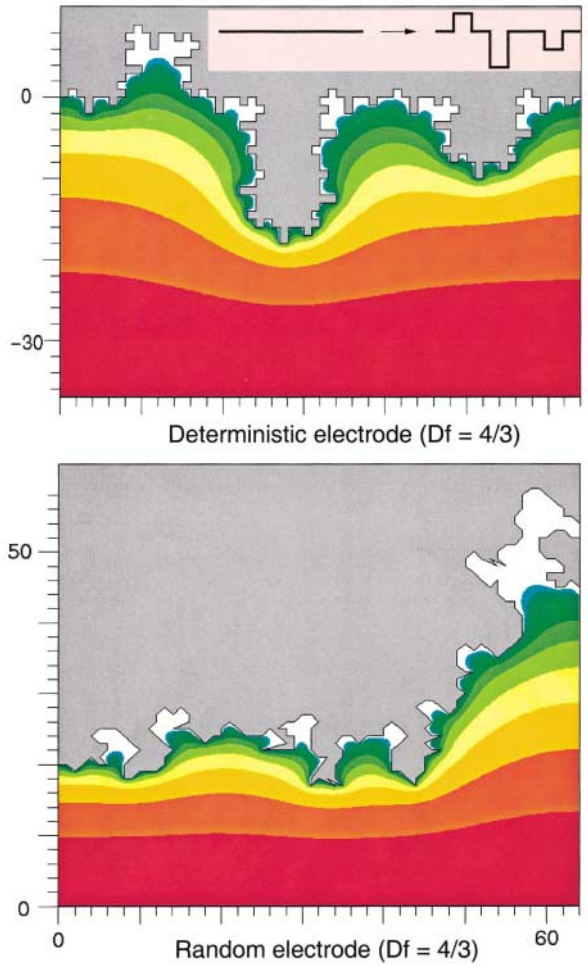

FIG. 5 (color). Isopotential curves for deterministic and random electrodes of fractal dimension $4/3$ with $\Lambda = 0$ (Dirichlet boundary condition). The generator for the deterministic electrode is shown on the top of the figure. Same color code as Fig. 4. The active zones are entirely different.

addressed in [9,11]. In this frame, the main parameters drawn from practical impedance spectroscopy measurements would be only the size, the perimeter, and the equivalent fractal dimension of the interface.

A more demanding comparison between the impedances can be made by comparing the values of r/Z as shown in Fig. 6. This quantity can be identified as an equivalent active length L_{eq} [12]. One finds three successives regimes, $\Lambda < l$, $l < \Lambda < L_p$, and finally $L_p < \Lambda$, separated by smooth crossovers. These regimes can easily be compared to the so-called "land surveyor approximation" [13]. This method allows one to compute Z_{spect} through a finite size renormalization of the interface geometry, without solving the Laplace equation. For small r (or $\Lambda \ll 1$), there is a linear regime in which Z_{spect} is proportional to r, that is, $Z_{\mathrm{spect}} = r/L_{\mathrm{eq}}$ with $L_{\mathrm{eq}} \approx L$ [9]. For values of $\Lambda > l$, there is a fractal regime in which, in first approximation, $Z_{\mathrm{spect}} = (r/\Lambda)\,(l/L)\,(\Lambda/l)^{1/D_f}$ and $L_{\mathrm{eq}} = L(\Lambda/l)^{(D_f-1)/D_f}$ (for more detailed expressions of

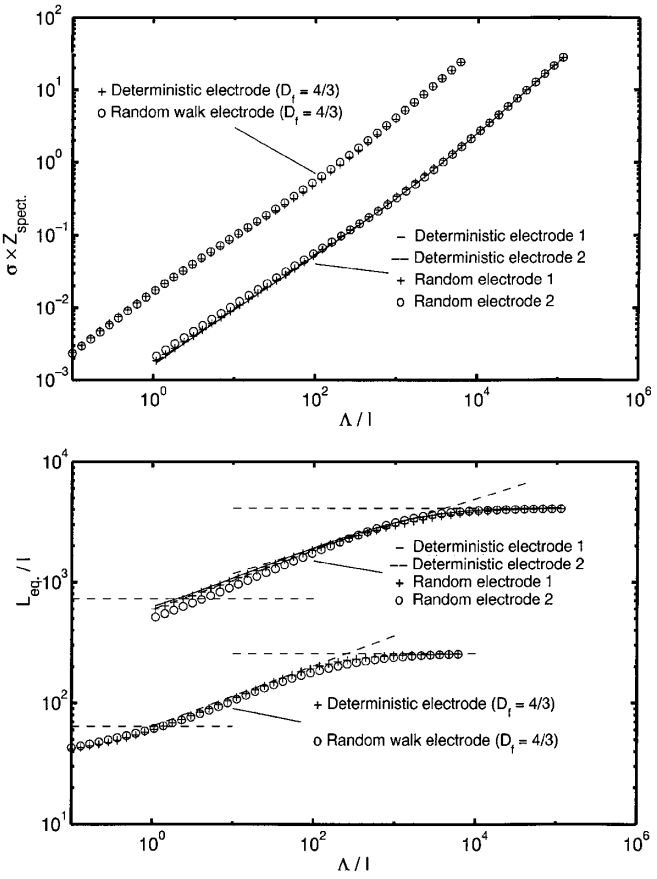

FIG. 6. Top: Plots of the electrode impedance Z_{spect} as a function of $\Lambda/l = r\sigma/l$, for various deterministic and random geometries. Note curve similarities despite very different current maps. Bottom: Plots of the "equivalent length" of the working surfaces defined by $L_{\text{eq}} = r/Z_{\text{spect}}$. Approximate expressions of Z_{spect} and L_{eq}, mentioned in the text, are indicated by the dashed lines.

the exponents, see [14–16]). Finally, for values of Λ much larger than the perimeter length L_p, the exact value is $Z_{\text{spect}} = r/L_p$ and $L_{\text{eq}} = L_p$. These three asymptotic behaviors are shown in the figure and are found to match the numerical results with good accuracy.

Note that the electrodes of Fig. 5 are in some sense "poor" fractals because the range of geometrical scaling is relatively small and it has been a matter of debate recently whether the fractal concept should be of any use when the scaling range of the geometry is too small. For the phenomena considered here, one can observe that the fractal description of this limited range geometry is really useful.

In summary, one has given several examples where the net transfer across an irregular surface is nearly independent of the randomness of its geometry, although it depends strongly on the geometry through its fractal dimension. The fact that the overall response remains the same indicates that, buried in the fractal description, there exist the geometrical correlations that govern the overall effect of screening *at different scales.* This result, obtained on two different types of randomness, suggests that the response could be universal within a very good approximation for a large class of fractal random geometries.

The authors wish to acknowledge useful discussions with P. Jones and N. Makarov. This research was supported by N.A.T.O. Grant No. C.R.G.900483. The Laboratoire de Physique de la Matière Condensée is "Unité Mixte de Recherches du Centre National de la Recherche Scientifique No. 7643."

[1] T. Vicsek, *Fractal Growth Phenomena* (World Scientific, Singapore, 1992).
[2] P. Meakin, *Fractals, Scaling and Growth Far from Equilibrium* (Cambridge University Press, Cambridge, England, 1998).
[3] B. B. Mandelbrot, *The Fractal Geometry of Nature* (Freeman, San Francisco, 1982).
[4] B. Sapoval, *Fractals* (Additech, Paris, 1989); *Universalité et fractales* (Flammarion, Paris, 1997).
[5] B. B. Mandelbrot and J. A. Given, Phys. Rev. Lett. **52,** 1853 (1984).
[6] L. de Arcangelis, S. Redner, and A. Coniglio, Phys. Rev. B **31**, 4725 (1985).
[7] B. Sapoval, in *Fractals and Disordered Systems*, edited by A. Bunde and S. Havlin (Springer-Verlag, Berlin, 1996), 2nd ed., p. 233.
[8] B. Sapoval, Phys. Rev. Lett. **73,** 3314 (1994).
[9] B. Sapoval, M. Filoche, K. Karamanos, and R. Brizzi, Eur. Phys. J. B **9**, 739 (1999). The word "spectroscopic" refers to impedance spectroscopy, which is the standard technique for measuring the electrode impedance.
[10] M. Bernadou *et al., Modulef: Une Bibliothèque Modulaire d'Éléments Finis* (INRIA, France, 1985).
[11] M. Filoche and B. Sapoval, Eur. Phys. J. B **9**, 755 (1999).
[12] Note that this length is different from the length of the active zone as defined in Refs. [9,11].
[13] M. Filoche and B. Sapoval, J. Phys. I (France) **7**, 1487 (1997).
[14] T. C. Halsey and M. Leibig, Ann. Phys. (N.Y.) **219,** 109 (1992); T. C. Halsey and M. Leibig, Phys. Rev. A **43,** 7087 (1991).
[15] R. C. Ball, in *Surface Disordering, Growth, Roughening and Phase Transitions*, edited by R. Julien, J. Kertesz, P. Meakin, and D. Wolf (Nova Science Publisher, Commack, NY, 1993), p. 277.
[16] H. Ruiz-Estrada, R. Blender, and W. Dieterich, J. Phys. Condens. Matter **6**, 10 509 (1994).